

## 6

# Atmospheric General Circulation and Climate

## 6.1 THE GREAT COMMUNICATOR

The movement of air in the atmosphere is of critical importance for climate. Atmospheric motions carry heat from the tropics to the polar regions and thereby reduce the extremes of temperature that would otherwise result. Water from the oceans is evaporated and carried in the air to land, where rainfall supports plant and animal life. Winds supply momentum to ocean surface currents that transport heat and oceanic trace constituents such as salt and nutrients. The circulation of the atmosphere is a key component of the climate, since it both responds to temperature and humidity gradients and helps to determine them by transporting energy and moisture. The atmosphere provides the most rapid communication between geographic regions within the climate system.

The global system of atmospheric motions that is generated by the uneven heating of Earth's surface area by the Sun is called the *general circulation*. A complete description of the atmosphere's general circulation includes mean winds, temperature and humidity, the variability of these quantities, and the covariances between wind components and other variables that are associated with large-scale weather systems. A statistical description of the general circulation of the atmosphere has been constructed from the ensemble of daily global flow patterns estimated with data from balloons and satellites. The general circulation of the atmosphere can be simulated by solving the equations of motion on a computer, and such general circulation models form a part of global climate models. The best estimates of the observed circulation of the atmosphere are constructed by combining observations with model equations as in an analysis to initialize a weather prediction model. For climate purposes, past data can be assimilated into a modern weather or climate prediction model using the best current model in a process called reanalysis, which

produces the best possible estimate of the time history of the atmospheric general circulation.

## 6.2 ENERGY BALANCE OF THE ATMOSPHERE

Atmospheric motions are generated by geographic variations in heating of the surface caused by meridional gradients of insolation, albedo variations, and other factors. These gradients in energy input produce gradients in energy content that is available to generate atmospheric motions. By transporting energy, winds generally act to offset the effects of these heating variations on atmospheric temperature. The local energy balance of an atmospheric column of unit horizontal area includes the effects of radiation, sensible and latent heat exchange with the surface, and the horizontal flux of energy in the atmosphere.

$$\frac{\partial E_a}{\partial t} = R_a + LE + SH - \Delta F_a \quad (6.1)$$

In (6.1),  $\partial E_a / \partial t$  is the time rate of change of the energy content of an atmospheric column of unit horizontal area extending from the surface to the top of the atmosphere,  $R_a$  is the net radiative heating of the atmospheric column,  $LE$  is the supply of latent heat to the atmosphere from surface evaporation,  $SH$  is the sensible heat transfer from the surface to the atmosphere, and  $\Delta F_a$  is the horizontal divergence of energy out of the column by transport in the atmosphere.

The net radiative heating of the atmosphere is the difference between the net downward irradiance at the top of the atmosphere and the net downward irradiance at the ground.

$$R_a = R_{TOA} - R_s \quad (6.2)$$

The storage of energy in the atmosphere is negligible, particularly when averaged over a year, so that the atmospheric energy balance is the sum of radiative heating, sensible heating, and latent heating, balanced against the export of energy by atmospheric motions.

$$R_a + LE + SH = \Delta F_a \quad (6.3)$$

The annually and zonally averaged net effect of radiative transfer on the atmosphere is a cooling of about  $-90 \text{ W m}^{-2}$ , which is nearly independent of latitude (Fig. 6.1). To balance this, evaporation provides about  $80 \text{ W m}^{-2}$  and sensible heat transfer about  $10 \text{ W m}^{-2}$ . The radiative cooling corresponds to an atmospheric temperature decrease of about  $1.5^\circ\text{C}$  per day (see Chapter 3). The energy lost from the atmosphere in 1 week

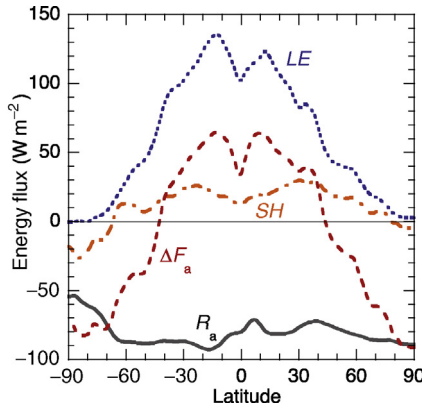


**FIGURE 6.1** Distribution with latitude of the components of the atmospheric energy balance averaged over longitude and over the annual cycle. Units are  $\text{Wm}^{-2}$ . Data from ERA-Interim.

through radiative transfer equals about 2.5% of the atmosphere's total energy content. If only the atmosphere's thermal capacity were considered, this cooling rate, acting alone, would bring the global mean surface air temperature to below freezing in about 2 weeks. Under normal circumstances, the radiative cooling is balanced in the global mean by heating from latent heat of condensation and sensible heat transfer from the surface.

Heating of the atmosphere by the transfer of sensible heat from the surface is relatively small. The largest contribution to balancing the radiative loss from the atmosphere is the supply of latent heat of vaporization from the surface, which is later converted to sensible heat during precipitation. In contrast to the radiative cooling, the addition of latent heat has a very distinctive structure with latitude peaking near  $140 \text{ Wm}^{-2}$  in the tropics and diminishing to near zero in high latitudes. The latitudinal structure of the evaporation is reflected in the latitudinal structure of the atmospheric energy flux divergence. Atmospheric motions export about  $50 \text{ Wm}^{-2}$  from the equatorial region and import about  $85 \text{ Wm}^{-2}$  into the polar regions. This poleward transport of energy by the atmosphere is one of the important climatic effects of the general circulation of the atmosphere.

## 6.3 ATMOSPHERIC MOTIONS AND THE MERIDIONAL TRANSPORT OF ENERGY

Motions in the atmosphere can be associated with many physical phenomena, which have a wide variety of space and time scales (Fig. 6.2). Small-scale phenomena such as turbulence and organized mesoscale phenomena such as thunderstorms are effective primarily at transporting

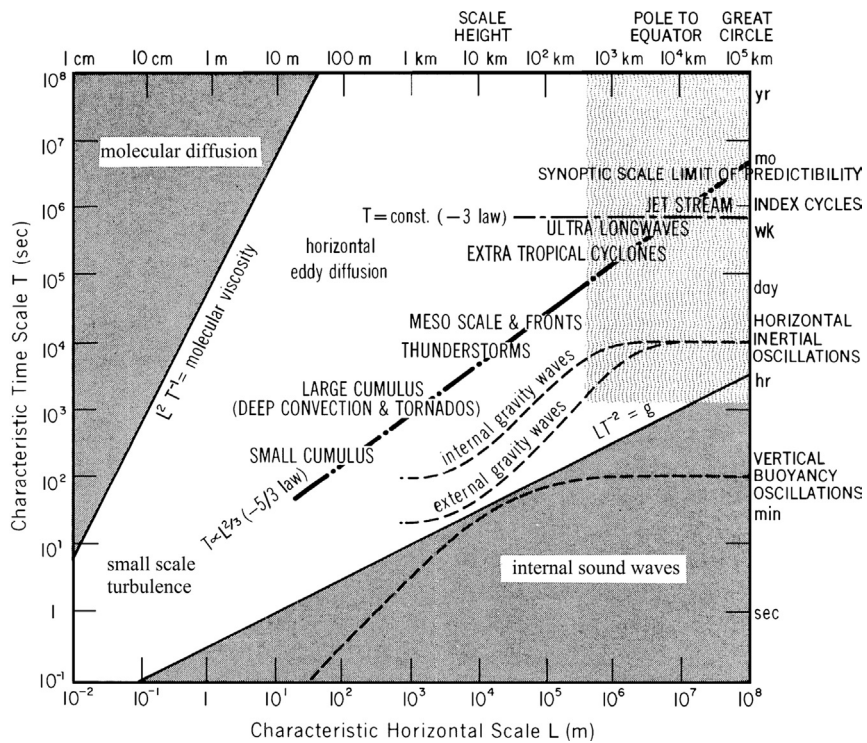


**FIGURE 6.2** The space and time scales of phenomena in the atmosphere. Light shading represents approximately scales that can be resolved in climate models. [From Smagorinsky (1974).]

momentum, moisture, and energy vertically. Only very large-scale phenomena such as extratropical cyclones, planetary-scale waves, and slow meridional circulations that extend over thousands of kilometers are effective at transporting momentum, heat, and moisture horizontally between the tropics and the polar regions. The upward flux of energy and moisture in the boundary layer and the poleward flux of energy by planetary-scale circulations in the atmosphere have equal importance for climate. These phenomena have characteristic spatial scales that differ by nearly 10 orders of magnitude: from millimeters to 10 thousand kilometers.

### 6.3.1 Wind Components on a Spherical Earth

Wind velocities in the atmosphere are measured in terms of a local Cartesian coordinate system inscribed on a sphere. At each latitude ( $\phi$ ) and longitude  $\lambda$  on a sphere of radius  $a$ , the zonal and meridional components of horizontal velocity are defined in the following way (Fig. 6.3):

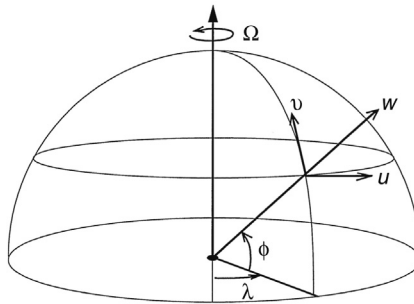


**FIGURE 6.3** Local Cartesian coordinates on a sphere and the zonal ( $u$ ), meridional ( $v$ ), and vertical ( $w$ ) components of the local vector wind velocity.

$$\begin{aligned} u &= a \cos \phi \frac{D\lambda}{Dt} = \text{zonal or eastward wind speed} \\ v &= a \frac{D\phi}{Dt} = \text{meridional or northward wind speed} \end{aligned} \quad (6.4)$$

Here  $D/Dt$  represents the material derivative – the temporal tendency that is experienced by an air parcel moving with the flow. The vertical component of velocity can be measured in terms of the rate of change of altitude, or the rate of change of pressure following the motion of air parcels.

$$\begin{aligned} w &= \frac{Dz}{Dt} = \text{rate of change of altitude following an air parcel} \\ \omega &= \frac{Dp}{Dt} = \text{rate of change of pressure following an air parcel} \end{aligned} \quad (6.5)$$

The vertical velocity and the pressure velocity are related to each other through an approximate equation, which is valid if a hydrostatic balance is maintained.

$$\omega \equiv -\rho g w \quad (6.6)$$

### 6.3.2 The Zonal Mean Circulation

In describing the circulations of the atmosphere, it is convenient to consider the zonal average, which is the average over longitude,  $\lambda$ , at a particular latitude and pressure, and is represented with square brackets.

$$[x] = \frac{1}{2\pi} \int_0^{2\pi} x d\lambda \quad (6.7)$$

Because of the relatively rapid rotation of Earth, and because diurnally averaged insolation is independent of longitude, averaging around a

latitude circle captures a physically meaningful subset of the climate. For climatological purposes, we are normally interested in averages over a period of time,  $\Delta t$ , that is long enough to average out most weather variations. This time interval may correspond to a particular month, season, or year, or it may be an average over an ensemble of many months, seasons, or years.

$$\bar{x} = \frac{1}{\Delta t} \int_0^{\Delta t} x dt \quad (6.8)$$

Climatological zonal averages are usually obtained by averaging over both longitude and time.

The distribution of the zonal mean of the eastward component of wind,  $u$ , through latitude and height is one of the best-known characterizations of the global atmospheric circulation, and is often called the *zonal mean wind* (Fig. 6.4). In meteorology, winds are called westerly when they flow from west to east and easterly when they flow from east to west, following

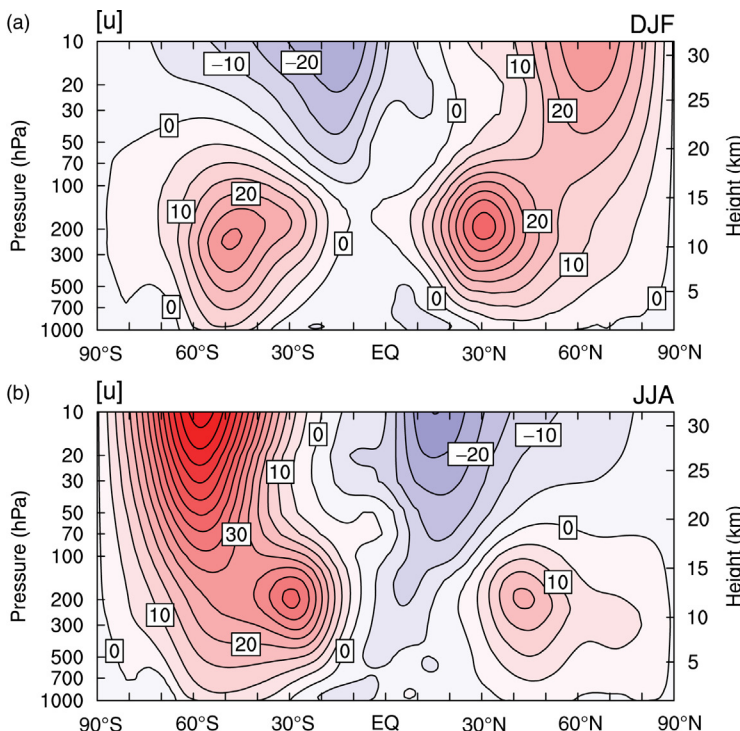


**FIGURE 6.4** Latitude-height cross-section of zonal-average wind speed for (a) DJF and (b) JJA. Contour interval is 5 m s<sup>-1</sup>; westerlies are red, easterlies are blue. Data from ERA-Interim.

nautical terminology. The zonal mean wind is westerly through most of the troposphere, and peaks at speeds in excess of  $30 \text{ ms}^{-1}$  in the subtropical jet stream, which is centered near  $30^\circ$  of latitude and at an altitude of about 12 km. The subtropical jet stream is strongest in the winter season. The zonal winds at the surface are westerly at most latitudes between  $30^\circ$  and  $70^\circ$ , but in the belt between  $30^\circ\text{N}$  and  $30^\circ\text{S}$  zonal mean easterly surface winds prevail. In the stratosphere, a strong westerly jet is present in the winter, stronger in the Southern Hemisphere, and shifts to easterlies in summer.

The zonal-average meridional and vertical components of wind are much weaker than the zonal wind. Maximum mean meridional winds are only about  $1 \text{ ms}^{-1}$ , and mean vertical wind speeds are typically a hundred times smaller than the mean meridional wind. The *mean meridional circulation* (MMC), which is composed of the zonal mean meridional and vertical velocities, can be described by a mass stream function, which is defined by calculating the northward mass flux above a particular pressure level,  $p$ .

$$\Psi_M = \frac{2\pi a \cos \phi}{g} \int_0^p [v] dp$$

The mass flow between any two streamlines of the mean meridional stream function is equal to the difference in the stream function values. The conservation of mass for the zonal mean flow implies a relationship between the mass stream function for the mean meridional circulation and the mean meridional velocity and pressure velocity.

$$[v] = \frac{g}{2\pi a \cos \phi} \frac{\partial \Psi_M}{\partial p} \quad (6.9)$$

$$[\omega] = \frac{-g}{2\pi a^2 \cos \phi} \frac{\partial \Psi_M}{\partial \phi} \quad (6.10)$$

Thus, the mean meridional velocity depends on the rate at which the stream function changes with pressure, and the zonal average pressure velocity depends on the rate at which the stream function changes with latitude.

The mean meridional circulation is dominated in the solstitial seasons by a single circulation cell in which air rises near the equator, flows toward the winter hemisphere at upper levels, and sinks in the subtropical latitudes of the winter hemisphere (Fig. 6.5). This mean meridional circulation cell is often called the *Hadley cell* after George Hadley, who in 1735 proposed it as an explanation for the trade winds. The mean meridional winds near the surface bring air back toward the equator. During the solstitial seasons the upward branch of the Hadley cell occurs in the summer

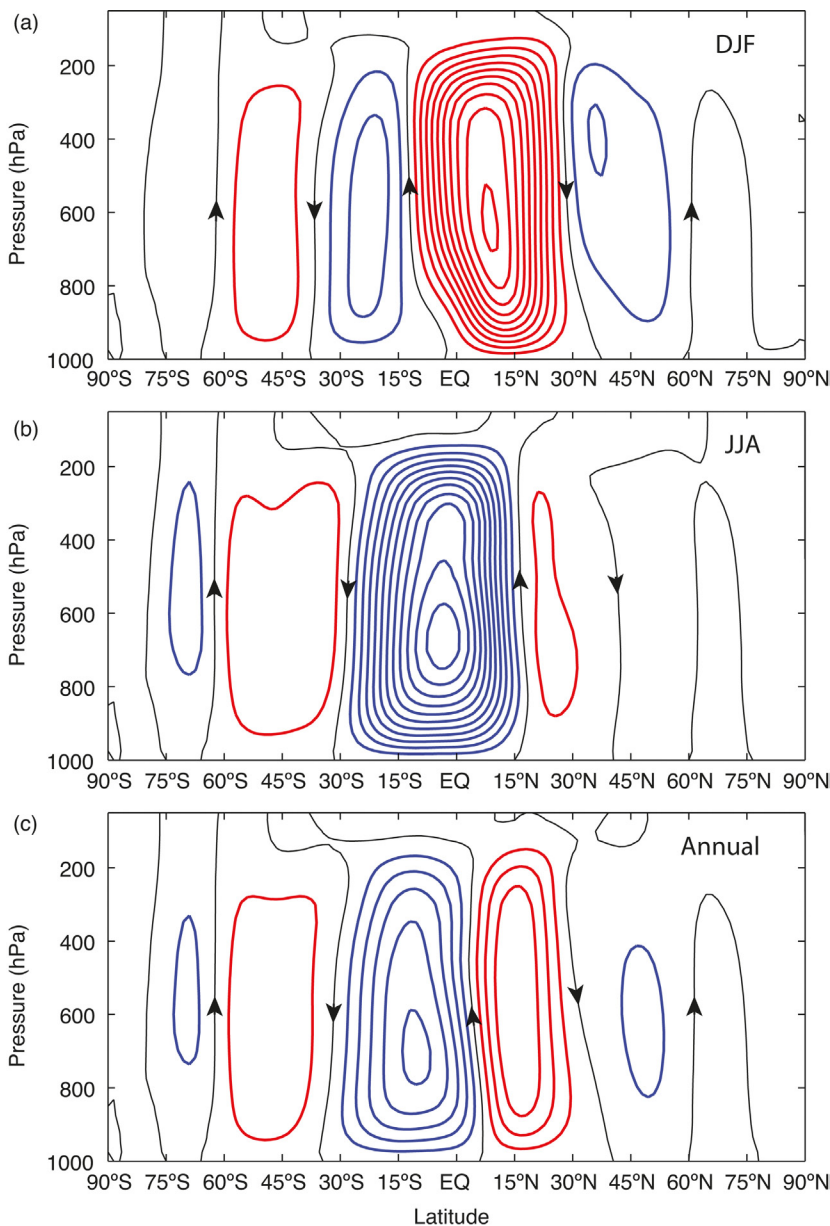


**FIGURE 6.5** Latitude-pressure cross-sections of the mean meridional mass stream function for the (a) DJF, (b) JJA, and (c) annual mean. Contour interval is  $2 \times 10^{10} \text{ kg s}^{-1}$  and the arrows on the zero contour indicate the direction of vertical motion. Red is positive and blue is negative. Based on ERA-Interim data.

hemisphere. In the annual mean, the rising branch is displaced slightly into the Northern Hemisphere, and the Hadley cell in the Southern Hemisphere is stronger. This asymmetry corresponds to a weak transport of energy from the Northern to the Southern Hemisphere.

In mid-latitudes, weaker cells called *Ferrel cells* circulate in the opposite direction to the Hadley cell. In these mid-latitude mean meridional circulation cells, rising occurs in cold air and sinking in warmer air. Therefore, these cells are thermodynamically indirect, in that they transport energy from a cold area to a warm area. The Ferrel cells are a by-product of the very strong poleward transport of energy and momentum by eddy circulations. Eddies are the deviations from the time or zonal average, and are a key component of the general circulation of the atmosphere. In mid-latitudes, eddies transport energy so efficiently that the mean meridional circulation is thermally indirect, with rising motion in cold air and sinking motion in warm air. The Ferrel cell in the Southern Hemisphere is stronger in the annual mean, because it persists in all seasons. Figure 6.6 shows the mean meridional mass stream function at 700 hPa as a function of season. This shows the greater strength and persistence of the Ferrel cell in the Southern Hemisphere, and also that during the equinoctial seasons, such as April and October, there are two weaker cells, one in each hemisphere.

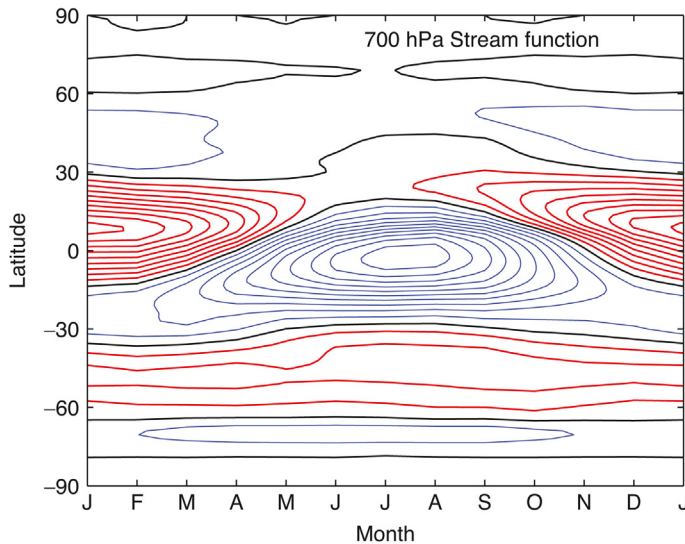


**FIGURE 6.6** Latitude-month cross-section of the mean meridional mass stream function at 700 hPa. Contour interval is  $2 \times 10^{10} \text{ kg s}^{-1}$ , northward overturning contours are red, southward turning contours are blue and the zero contour is black. Based on ERA-Interim data.

### 6.3.3 Eddy Circulations and Meridional Transport

The cyclones and anticyclones that are responsible for most of the weather variations in mid-latitudes produce large meridional transports of momentum, heat, and moisture. These disturbances have large wind and temperature variations on scales of several thousand kilometers, which do not appear in a zonal average, but have a profound effect on the zonal mean climate. The fluctuations associated with weather appear as deviations from the time average.

$$x' = x - \bar{x} \quad (6.11)$$

In addition to temporal variations associated with mid-latitude cyclones, the atmosphere exhibits variations around latitude circles associated with continents and oceans that are quasi-stationary and appear clearly in time averages. These are characterized by the deviations of the time mean from its zonal average.

$$\bar{x}' = \bar{x} - [\bar{x}] \quad (6.12)$$

Northward eddy fluxes of temperature are produced when northward-flowing air is warmer than southward-flowing air, so that, when averaged over longitude, the product of meridional velocity and temperature is positive, even when the mean meridional wind is zero. Using the definitions of the time and zonal averages, the northward transport of temperature averaged around a latitude circle and over time can be written as the sum of contributions from the mean meridional circulation, the stationary eddies, and the transient eddies, which are shown respectively as the three terms on the right of (6.13).

$$[\bar{v}\bar{T}] = [\bar{v}][\bar{T}] + [\bar{v}'\bar{T}'] + [\bar{v}'T'] \quad (6.13)$$

Transient eddy fluxes are associated with the rapidly developing and decaying weather disturbances of mid-latitudes, which generally move eastward with the prevailing flow and contribute much of the variations of wind and temperature, especially during winter. These disturbances are very apparent on weather maps and have typical periods of several days to 1 week.

The positive correlation between poleward velocity and temperature in large-scale atmospheric waves results from the tendency of the temperature wave to be displaced westward relative to the pressure wave, especially in the lower troposphere (Fig. 6.7). This arrangement is associated with a conversion from energy available in the mean meridional temperature gradient to the energy of waves. Cyclone waves whose amplitude is increasing rapidly with time have a large zonal phase shift between their pressure and temperature waves, and thus produce efficient poleward transports of heat and moisture.

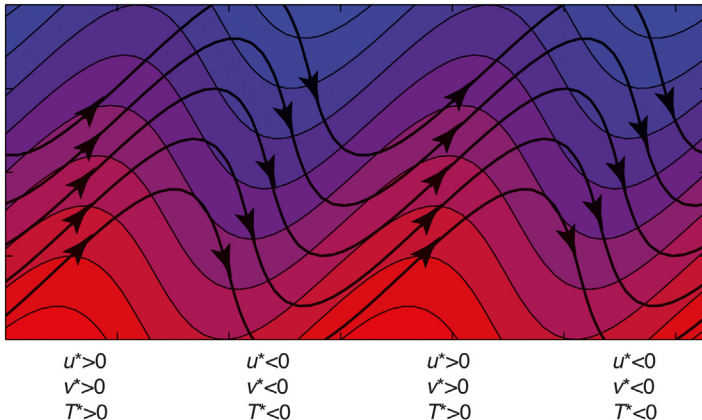


**FIGURE 6.7** Schematic of the streamlines (black with arrows) and isotherms (colors) associated with a large-scale atmospheric disturbance in mid-latitudes of the Northern Hemisphere. Arrows along the streamline contour indicate the direction of wind velocity. The streamlines correspond approximately to lines of constant pressure, since the winds are nearly geostrophic. The signs of the deviations of the wind components and temperature from their zonal average values are shown with asterisks to illustrate that the NE-SW tilt of the streamlines indicates a northward zonal momentum transport, and the westward phase shift of the temperature wave relative to the pressure wave gives a northward heat transport.

Eddy fluxes by the time-averaged flow are associated with stationary planetary waves. *Stationary planetary waves* are departures of the time average from zonal symmetry and are plainly visible in monthly mean tropospheric pressure patterns (Fig. 6.8). They result from the east–west variations in surface elevation and surface temperature associated with the continents and oceans. Stationary eddy fluxes are largest in the Northern Hemisphere where the Himalaya and Rocky Mountain ranges provide mechanical forcing of east–west variations in the time mean winds and temperatures. The thermal contrast between the warm waters of the Kuroshio and Gulf Stream ocean currents and the cold temperatures in the interiors of the continents also provides strong thermal forcing of stationary planetary waves during winter.

The poleward fluxes of temperature by stationary and transient eddies peak at about  $50^\circ$  of latitude in the winter hemisphere in the lower part of the troposphere (Fig. 6.9). The low-level maximum is associated with the structure of growing extratropical cyclones, in which the phase difference between temperature and pressure is largest in the lower troposphere. The fluxes exhibit a minimum near the tropopause and then increase with height into the winter stratosphere. Temperature fluxes have a large seasonal variation in the Northern Hemisphere, with large values in winter and fairly small values during summer. In the Southern Hemisphere, the seasonal contrast is less, since the Southern Hemisphere is mostly ocean,

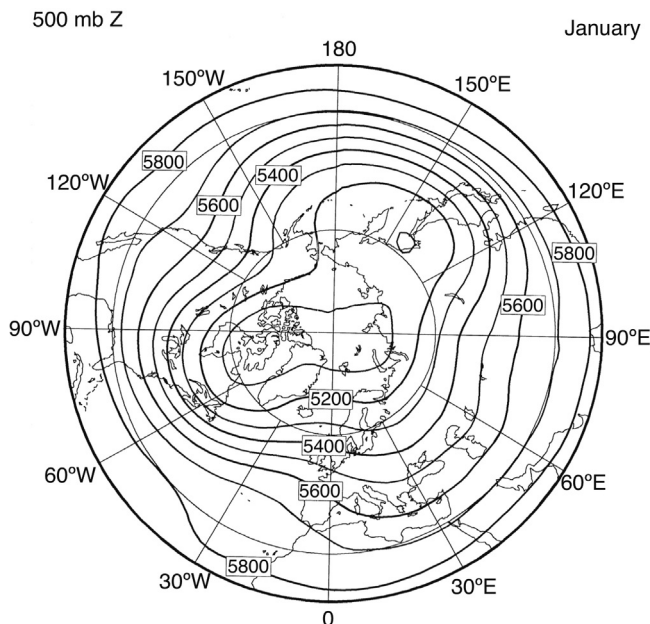


**FIGURE 6.8** Average height of the 500 hPa pressure surface during January in the Northern Hemisphere. Contour interval 100 m.

which has large heat capacity. Transient eddy fluxes dominate the meridional flux of temperature except in the Northern Hemisphere during winter, when stationary eddies contribute up to half of the flux.

#### 6.3.4 Meridional Water Flux in the Atmosphere

The mean meridional circulation and eddies transport water and play an important role in determining the nature of the hydrologic cycle. Atmospheric eddies move water vapor from the tropics and supply it to middle and high latitudes (Fig. 6.10). The transport of vapor occurs mostly in the lower troposphere where the specific humidity is larger. The left panel of Fig. 6.11 shows the vertically integrated northward transport of water vapor, including the contributions from the mean meridional circulation and from eddies. In the tropics, the mean meridional circulation dominates the total transport, with moisture transported toward the equatorial region by the trade winds. Since the southern branch of the Hadley cell is stronger, the transport of moisture is northward at the equator toward the intertropical convergence zone (ITCZ), whose average position is north of the equator. In the extratropics, the poleward transport is dominated by eddies. The meridional convergence of atmospheric moisture transport in

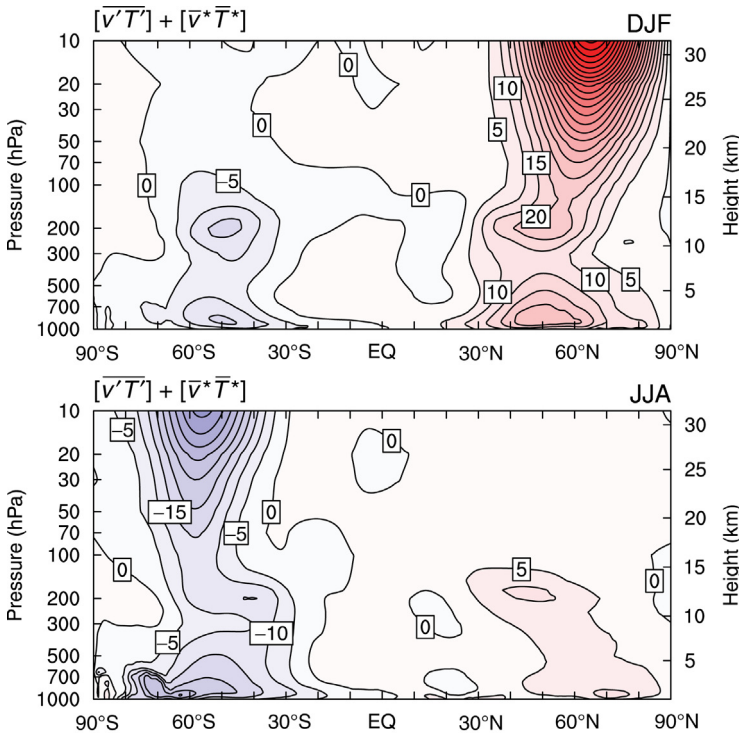


**FIGURE 6.9** Meridional cross-section of the zonally averaged northward flux of temperature by eddies. Note that in the Southern Hemisphere the poleward fluxes are negative (blue shading) as a result of our arbitrarily defining north as the positive direction. Contour interval is  $5 \text{ K ms}^{-1}$ . Data from ERA Interim.

the tropics is also dominated by the transport provided by the mean meridional circulation, which produces a total convergence of moisture in the equatorial region of about  $4 \text{ mm day}^{-1}$  ( $1.5 \text{ m year}^{-1}$ ) that is supplied from the subtropics (right panel of Fig. 6.11). The eddies draw moisture from the tropics and deliver it to middle and high latitudes. In the Northern Hemisphere, moisture is converged almost uniformly in the region from  $40\text{--}90^\circ\text{N}$ , but in the Southern Hemisphere, moisture converges more strongly in the belt from  $40\text{--}70^\circ\text{S}$  because of the presence of the high continent of Antarctica.

### 6.3.5 Vertically Averaged Meridional Energy Flux

Four types of atmospheric energy are important for determining the meridional transport of energy (Table 6.1). Internal energy is the energy associated with the temperature of the atmosphere, and potential energy

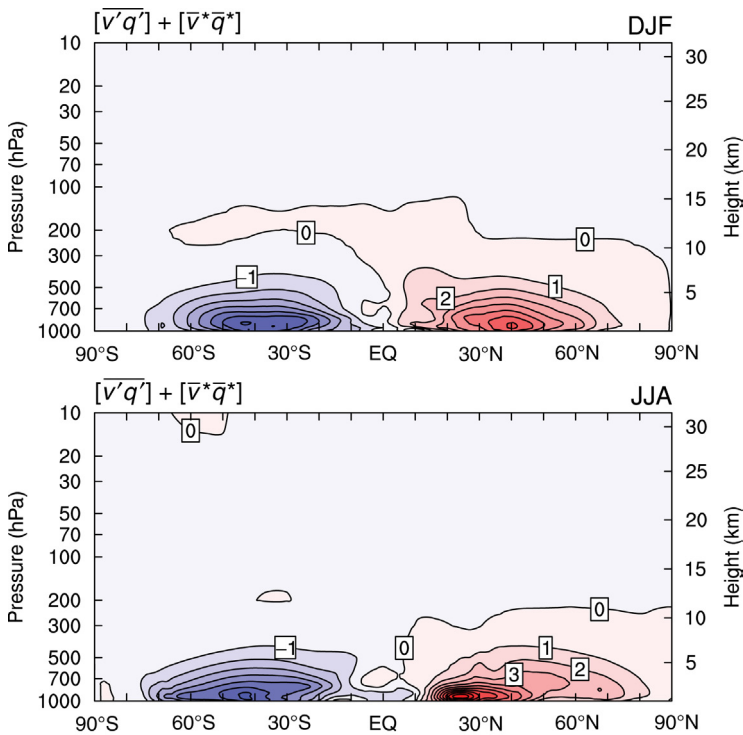


**FIGURE 6.10** Meridional cross-section of the zonally averaged northward flux of water vapor by eddies. Contour interval is  $1 \text{ g kg}^{-1} \text{ m s}^{-1}$ . Northward transport is shaded red. Data from ERA Interim.

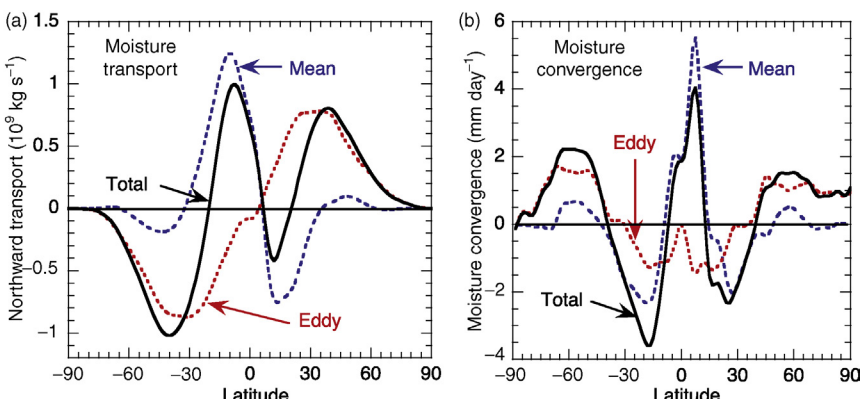


**FIGURE 6.11** Meridional transport of moisture in  $10^9 \text{ kg s}^{-1}$  (a) and convergence of meridional transport of moisture in  $\text{mm day}^{-1}$  (b); totals and contributions by the mean meridional circulation and eddies are shown. Data from ERA Interim reanalysis.

**TABLE 6.1** Kinds and Amounts of Energy in the Global Atmosphere

Name	Symbol	Formula	Amount ( $\text{J m}^{-2}$ )	Total (%)
Internal energy	IE	$c_v T$	$1800 \times 10^6$	70
Potential energy	PE	$gz$	$700 \times 10^6$	27
Latent energy	LH	$Lq$	$70 \times 10^6$	2.7
Kinetic energy	KE	$1/2(u^2 + v^2)$	$1.3 \times 10^6$	0.05
Total energy	IE + PE + LH + KE		$2571 \times 10^6$	100

is the energy associated with the gravitational potential of air some distance above the surface. Together internal and potential energy constitute about 97% of the energy of the atmosphere. Although kinetic energy comprises a small fraction of the total energy, it is still very important to understand its generation and maintenance, because the motions are the means by which energy is transported from equator to pole. Motions are also important in converting one form of energy to another. Furthermore, most of the internal and potential energy is unavailable for conversion into other forms. For example, in a dry, hydrostatic atmosphere without mountains, one can show that the ratio of the potential energy to the internal energy is  $R/c_v = 0.4$ . This simple relation between internal and potential energy reflects the fact that much of the internal energy of the atmosphere is required simply so that the atmosphere may “hold itself up” against gravity, and is not available for generating motion.

Insolation drives the circulation by heating the tropics more than the polar regions. Winds are driven by the density and pressure gradients generated by this uneven heating. The circulation responds not to the total amount of energy in the atmosphere, but to the temperature gradients on constant pressure surfaces. For this reason, the maximum kinetic energy occurs during winter, when the meridional temperature gradients are strongest, and not in the summer, when the total amount of energy in the atmosphere is greatest.

The meridional transport of energy by the atmosphere may be divided into contributions from sensible, geopotential and latent forms that comprise the moist static energy.

$$\text{Moist static energy} = c_p T + gz + Lq = \text{sensible} + \text{potential} + \text{latent} \quad (6.14)$$

Here  $g$  is the acceleration of gravity,  $z$  is altitude,  $q$  is the mass-mixing ratio of water vapor, and  $L$  is the latent heat of vaporization. Moist static energy is moved around by the motions of the atmosphere and these transports can be integrated through the mass of the atmosphere to reveal the total meridional flux of energy in various forms (Fig. 6.12). Although

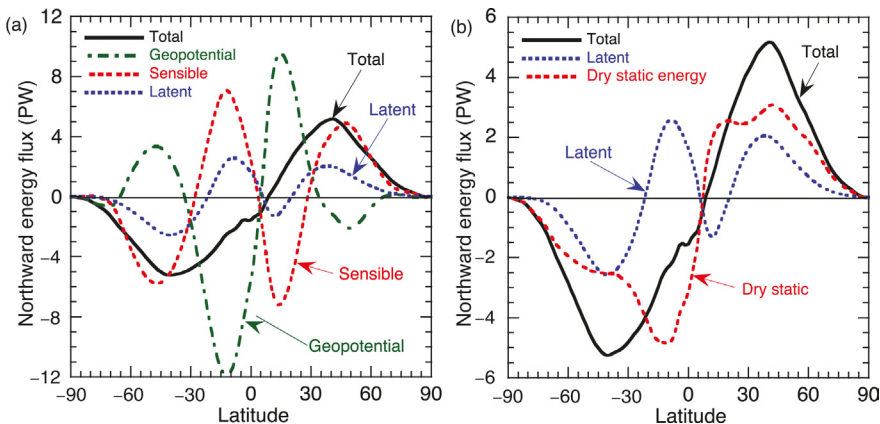


**FIGURE 6.12** Northward transport of energy by the atmosphere in potential, sensible and latent forms. In (b), geopotential and sensible heat fluxes have been combined to form the dry static energy transport. Units are  $10^{15}$  W. Data from ERA Interim.

the total moist static energy transport is smoothly poleward in both hemispheres, the individual components change sign and often strongly offset each other. If the sensible and geopotential transports are combined to form the dry static energy transport, then it can be seen that the transport of latent heat is equally important to the dry static energy transport in mid-latitudes, especially in the Southern Hemisphere. The total transport is negative at the equator, so that the atmosphere transports energy from the Northern Hemisphere to the Southern Hemisphere in the annual mean. This southward energy transport at the equator is related to the fact that the Hadley cell rises in the Northern Hemisphere, as mentioned previously. In Fig. 2.14 we noticed that radiation budget measurements indicated a net northward energy transport at the equator, which requires a northward transport by the ocean to offset the southward transport by the atmosphere. Therefore, it seems likely that northward transport by the ocean at the equator is requiring southward transport by the atmosphere there. The seasonal variation of the northward energy transport is shown in Fig. 6.13. The strong role of the Hadley circulation near the equator is very apparent in the seasonal and latitudinal distributions of northward flux of geopotential, sensible, and latent energy. The Hadley cell influence on the total energy is less obvious because of the cancellation between energy fluxes. Poleward energy transports are largest in mid-latitudes and peak strongly in winter when the radiative forcing of meridional temperature gradients is greatest. The seasonal variation is larger in the Northern Hemisphere, where more land is present.

The cancellation between the transports of different types of energy is particularly strong in the Hadley circulation. The net transport in the

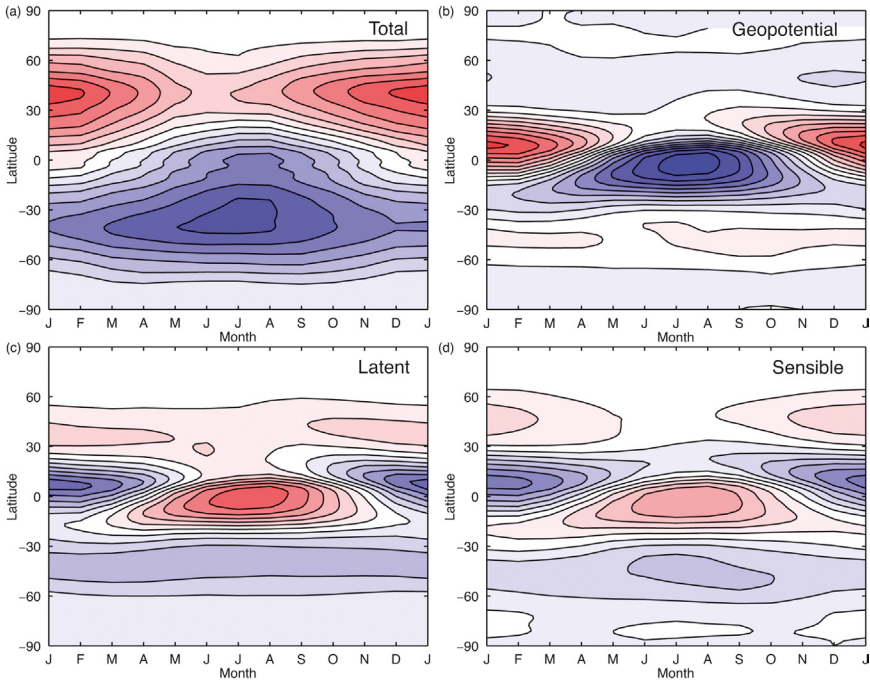


**FIGURE 6.13** Contour plots of the vertically integrated (a) total, (b) potential, (c) sensible and (d) latent northward energy transport as functions of latitude and season. Red shading indicates northward transport and blue shading southward transport. Contour interval is 1 PW for total and latent and 3 PW for potential and sensible energy.

Hadley cell is only about 10% of the potential energy transport. Mean meridional circulation cells are not a particularly efficient means of poleward energy transport, especially in view of the strong constraints the angular-momentum balance places on these circulation cells. The Hadley cell transports both sensible and latent heat equatorward in the tropics. The equatorward flow near the surface brings warm moist air with it. Heavy precipitation occurs where warm moist air converges in the vicinity of the equator. The release of latent heat and the convergence of sensible heat flux drive strong rising motion in the upward branch of the Hadley cell. In the upward branch of the Hadley cell, latent and internal energy are converted into potential energy. The poleward flow of potential energy in the upper branch of the Hadley cell exceeds the sum of the equatorward flow of latent and internal energy in the lower branch, giving a small net poleward flow of energy. The poleward flow of energy in the Hadley cell can be better visualized by considering the vertical distribution of moist static energy, which is the sum of sensible, potential, and latent energy (Fig. 6.14). Sensible and latent heat per unit mass both peak near the

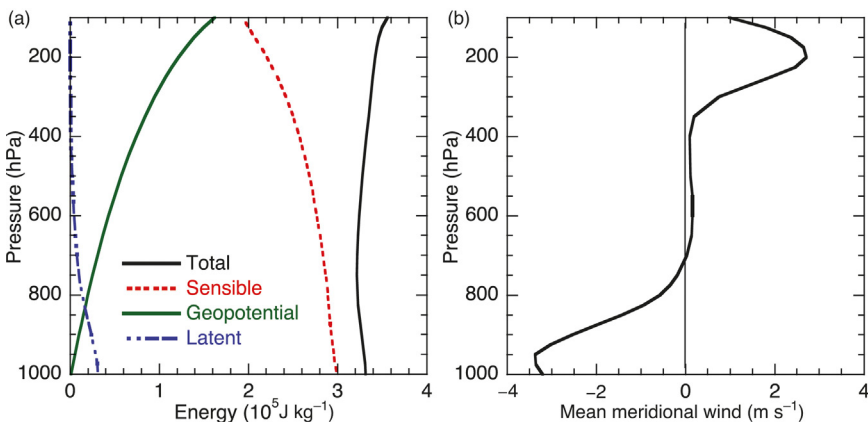


**FIGURE 6.14** Zonal mean energy content (a) and mean meridional velocity (b) at 13.5°N plotted versus pressure. This shows why the mean meridional circulation transports sensible and latent energy toward the equator, but potential and total moist static energy toward the pole.

surface and so are transported in the direction of the lower branch of the Hadley cell. In the upper troposphere, the Hadley cell transports potential energy poleward, giving a small poleward transport of moist static energy.

## 6.4 THE ANGULAR-MOMENTUM BALANCE

The general circulation of the atmosphere is heavily constrained by the conservation of angular momentum. *Angular momentum* is the product of mass times the perpendicular distance from the axis of rotation times the rotation velocity. The angular momentum about the axis of rotation of Earth can be written as the sum of the angular momentum associated with Earth's rotation, plus the angular momentum of zonal air motion measured relative to the surface of Earth. Because the depth of the atmosphere is so thin compared to the radius of Earth, the altitude in the atmosphere is unimportant for the angular momentum of the air, and we may use a constant radius,  $a$ , to describe the distance from the center of Earth. The latitude has a strong influence on the angular momentum, however, because increasing latitude decreases the distance to the axis of rotation (Fig. 6.15). The distance to the axis of rotation is the radius of Earth times the cosine of latitude. The zonal velocity consists of the velocity of Earth's surface associated with rotation plus the relative zonal velocity of the wind.

$$M = (\Omega a \cos \phi + u)a \cos \phi = (u_{\text{earth}} + u)a \cos \phi \quad (6.15)$$

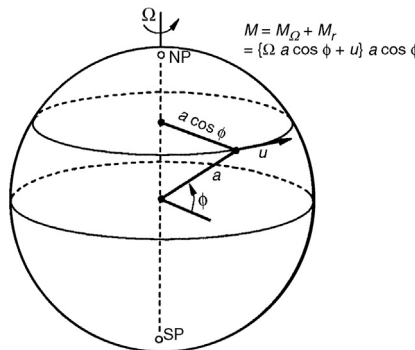


**FIGURE 6.15** The component of angular momentum about the axis of rotation of Earth. From Peixoto and Oort (1984) with permission from the American Physical Society.

The zonal velocity of Earth's surface at the equator, about  $465\text{ ms}^{-1}$ , is very large compared to typical zonal wind speeds in the atmosphere.

$$\begin{aligned} u_{\text{earth}} &= \Omega a \cos \phi = 7.292 \times 10^{-5} \text{ rads}^{-1} \times 6.37 \times 10^6 \text{ m} \cdot \cos \phi \\ &= 465 \text{ ms}^{-1} \times \cos \phi \end{aligned}$$

The atmospheric angular momentum associated with Earth's rotation is thus much larger than the angular momentum associated with the zonal winds normally observed in the troposphere. When air parcels move poleward in the atmosphere, they retain the same angular momentum unless they exchange angular momentum with other air parcels or with the surface. Since the distance to the axis of rotation of Earth decreases as a parcel moves poleward on a level surface, the relative eastward zonal velocity of the parcel must increase to maintain a constant total angular momentum. Thus, poleward-moving parcels experience an eastward acceleration relative to Earth's surface.

If a parcel of air moves from one latitude to another while conserving angular momentum, then (6.15) implies a relationship between the zonal velocities the parcel will have at any two latitudes.

$$M = (\Omega a \cos \phi_1 + u_1) a \cos \phi_1 = (\Omega a \cos \phi_2 + u_2) a \cos \phi_2 \quad (6.16)$$

If a parcel starts out at the equator with zero relative velocity and moves poleward to another latitude while conserving its angular momentum, we have from (6.16) that

$$M = \Omega a^2 = (\Omega a \cos \phi + u_\phi) a \cos \phi \quad (6.17)$$

which can be rearranged to yield an expression for the zonal velocity at any other latitude  $u_\phi$ ,

$$u_\phi = \Omega a \frac{\sin^2 \phi}{\cos \phi} \quad (6.18)$$

By substituting numbers into (6.18) we find that a parcel of air with the angular momentum of Earth's surface at the equator will have a westerly zonal wind speed of  $134 \text{ ms}^{-1}$  at  $30^\circ\text{N}$  or  $30^\circ\text{S}$ . This is much greater than the maximum zonally averaged wind speeds in the subtropical jet stream (Fig. 6.4), and we infer that the poleward angular momentum transport in the upper, poleward-flowing branch of the Hadley cell is more than adequate to explain the existence of a  $40 \text{ ms}^{-1}$  jet at  $30^\circ$  latitude. The interesting part is explaining why the subtropical jet stream is not stronger than it is. A parcel traveling at a mean meridional velocity of  $1 \text{ ms}^{-1}$  would require about 30 days to travel from the equator to  $30^\circ\text{N}$ , allowing plenty of time for small-scale turbulence or some other slow process to reduce the angular momentum of the parcel. In fact, drag by small-scale eddies is probably not the most important mechanism for reducing the angular momentum of air parcels in the upper branch of the Hadley cell. Rather it is the large-scale eddies in the atmosphere that transport momentum out of the Hadley cell, into mid-latitudes, and downward to the surface.

The zonally averaged meridional flux of angular momentum in the atmosphere can be written

$$\overline{[vM]} = \overline{[\bar{v}](\Omega a \cos \phi + [\bar{u}])a \cos \phi + [\bar{u}'v']} + [\bar{u}'\bar{v}'] a \cos \phi \quad (6.19)$$

and consists of the transport of the zonal mean angular momentum by the mean meridional velocity and an eddy flux term that depends on the covariance between zonal and meridional velocity fluctuations around a latitude circle. This eddy flux term becomes the dominant one near  $30^\circ$  latitude, where the mean meridional velocity is small. The eddy flux of zonal momentum peaks at about the tropopause level at  $35^\circ$  latitude, where it is poleward in both hemispheres and strongest in the winter season (Fig. 6.16).

Northward zonal momentum flux by large-scale atmospheric disturbances is produced when the streamlines of the flow are oriented such that high and low anomalies tilt from southwest to northeast in the Northern Hemisphere as illustrated in Fig. 6.7. It can be seen that when the streamlines are tilted in this manner, the eastward component of wind is greater when the meridional wind component is poleward, and the eastward component of wind is weaker when the meridional flow is equatorward. Therefore, an average over longitude of the product of the deviations of the zonal and meridional components of wind will be positive, indicating a northward flux of zonal angular momentum.

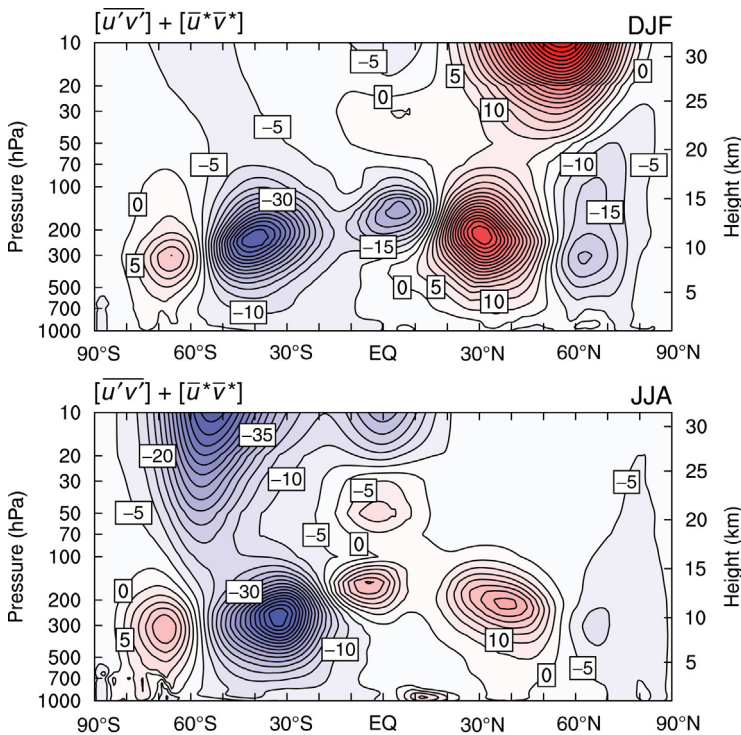


**FIGURE 6.16** Zonal cross-section of the northward transport of zonal velocity by eddies. Contour interval is  $5 \text{ m}^2 \text{ s}^{-2}$ , and red shading is northward transport.

The flow of angular momentum in the atmosphere is shown schematically in Fig. 6.17. In the tropical surface easterlies, where the atmosphere rotates more slowly than Earth's surface, eastward angular momentum is transferred from Earth to the atmosphere via frictional forces and pressure forces acting on mountains. This westerly angular momentum is transported upward and then poleward in the Hadley cell. Atmospheric eddies transport angular momentum poleward and downward into the mid-latitude westerlies. Where the surface winds are westerly, the atmosphere is rotating faster than Earth's surface and the eastward momentum is returned to Earth. It is clear that the surface zonal winds cannot be of the same sign everywhere, since eastward angular momentum must flow into the atmosphere where the surface winds are easterly, and must return to Earth where the surface winds are westerly. Thus the tropical easterly winds and mid-latitude westerlies that so regulate the routes of sailing ships are required to satisfy the angular momentum constraint on atmospheric flow.

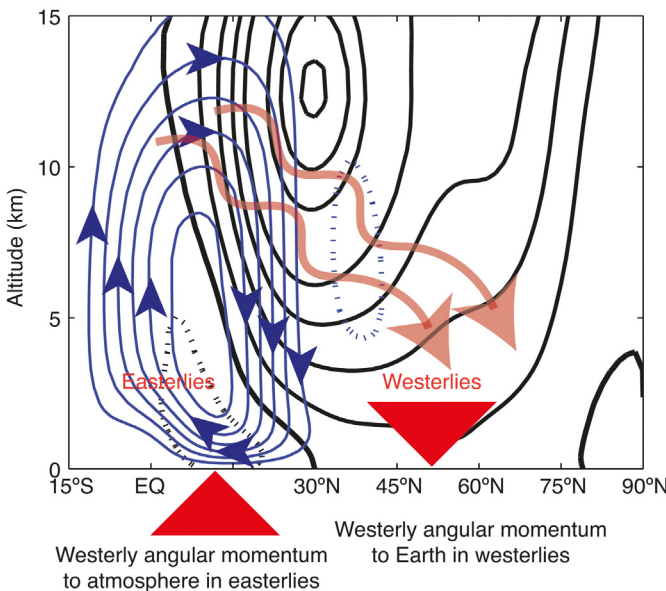


**FIGURE 6.17** Schematic illustration of the flow of angular momentum from the Earth through the atmosphere and back to Earth. Blue contours with arrows are the mean meridional stream function. Solid black lines are zonal mean wind. Dotted contours indicate negative values of zonal wind and stream function. Wavy arrows indicate poleward and downward angular momentum transport by eddies. Wind and stream function are for January.

## 6.5 LARGE-SCALE CIRCULATION PATTERNS AND CLIMATE

The circulation of the atmosphere is not zonally symmetric, and east–west variations of winds and temperature are important for regional climates. For example, the subtropical jet of mid-latitudes is not equally strong at all longitudes, but has local maxima associated with the distribution of land and ocean (Fig. 6.18). During January in the Northern Hemisphere the subtropical jet stream has two local wind speed maxima downstream of the Tibetan Plateau and Rocky Mountains over the Pacific and Atlantic oceans, respectively. These maxima in the time-average wind speed have maxima in the transient eddy activity and eddy fluxes of heat and moisture associated with them. They define the so-called *storm tracks*, where vigorous mid-latitude cyclones are most frequently observed. The seasonal migration of these storm tracks plays a key role in the annual variation of precipitation along the west coast of North America discussed in Chapter 5. During July, the wind maximum of mid-latitudes is weaker and farther poleward in the Northern Hemisphere. In the Southern Hemisphere, the mid-latitude jet at about 50°S is present in all seasons, but the

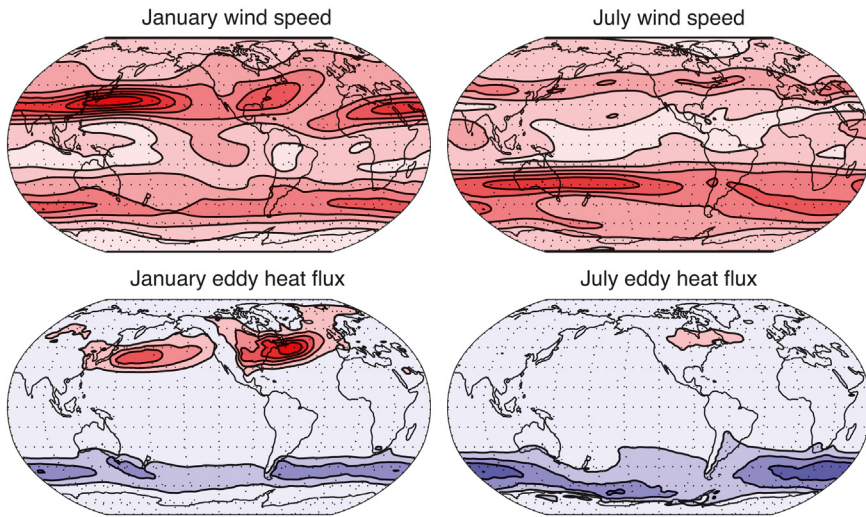


**FIGURE 6.18** Average wind speed (top) and northward heat flux by eddies with periods shorter than about 1 week. Contour interval on the top is  $10 \text{ ms}^{-1}$  and contour on the bottom is  $5 \text{ Km s}^{-1}$ , zero contours are not shown and blue shading indicates southward transport. Robinson projection is used. Data from ERA Interim.

subtropical jet is strongest in July (winter) and located in the Western Pacific and over Australia, where strong convection over Indonesia drives a localized Hadley circulation. The extratropical jet and associated transient eddy heat fluxes are concentrated in the Atlantic and Indian Ocean sectors and are weakest in the Pacific sector. The Southern Hemisphere storm track is thus stronger in the Atlantic and Indian oceans in both winter and summer. The seasonal variation of transient eddy heat fluxes is much stronger in the Northern Hemisphere.

The distribution of surface air pressure is an important indicator of the general circulation. In Fig. 6.19, the height of the 1000 hPa surface is shown as a smooth proxy for surface pressure. The global mean value of about 16 m has been removed. Near the surface, air tends to spiral inward toward low-pressure centers, as is clearly indicated for the mid-latitude low-pressure centers over the Pacific and Atlantic oceans during January. By the conservation of mass, this converging air must rise over the low-pressure center. Conversely, the flow near the surface spirals outward from high-pressure centers, so that high pressure is generally indicative of subsiding motion above the boundary layer and suppressed convection. The surface pressure near  $30^\circ$  latitude is generally higher than the surface pressure at the equator. This is consistent with the surface trade winds of the tropics, which generally blow toward the equator from both hemispheres and meet in the ITCZ near the equator, where the surface pressure is low and

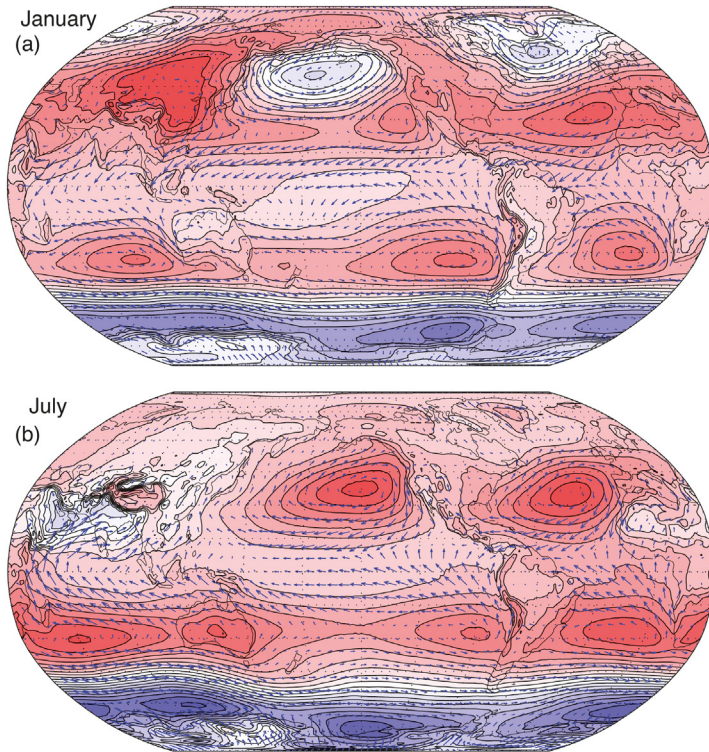


**FIGURE 6.19** 1000 hPa height and wind vectors for (a) January and (b) July. Contour interval is 20 m and largest vector represents a wind of about  $15 \text{ ms}^{-1}$ . Positive heights are in red. Data from ERA Interim.

where deep convection occurs with its attendant latent heat release and large-scale upward motion.

The seasonal variations in sea-level pressure are most apparent in the Northern Hemisphere. During January, the high-latitude oceans are characterized by low-pressure centers with the Aleutian and Icelandic lows centered in the northern margins of the Pacific and Atlantic oceans, respectively. A high-pressure center lies over Asia. During July, the land–sea pressure contrast is reversed in mid-latitudes, with the highest pressures over the oceans and the lowest pressures over the land areas. The oceanic highs are centered over  $40^\circ\text{N}$ , compared to their position at about  $30^\circ\text{N}$  during January. The dominant low-pressure feature during Northern Hemisphere summer is centered over Asia at about  $30^\circ\text{N}$ , and is associated with the Asian summer monsoon.

The dramatic shifts in land–sea pressure distribution are driven by seasonal changes of insolation and the different responses of the land and ocean to heating. Over the oceans the response of surface temperature to

seasonal variations of insolation is smaller because the energy is put into a deep layer of ocean with a large heat capacity and because evaporation consumes much of the heat input. Land surfaces have a much smaller capacity for storing heat, and often are not sufficiently wet that evaporation can balance large summertime increases in insolation. As a result, the land surfaces warm up dramatically in summer and cool in winter. The pressure variations along latitude circles in mid-latitudes are associated with the dynamical response to the land–sea temperature and heating contrasts. The low pressures generally occupy the warm regions where the atmosphere is heated, and the high pressures occur where the temperature is low and the atmosphere is being cooled. Land surfaces are warmer than adjacent oceans in summer and are colder than the oceans during winter (see Fig. 1.6).

### 6.5.1 Monsoonal Climates

The seasonal movement of maximum insolation from one hemisphere to the other causes seasonal shifts in the tropical winds and precipitation, which have dramatic effects on the populations there. In some regions of the tropics, the winds blow consistently in one direction during part of the year and then may weaken or blow from a very different direction for the rest of the year. Such regular seasonal changes in wind speed and direction are called monsoons. The word *monsoon* is derived from an Arabic word meaning season. In many parts of Africa, Asia, and Australia, seasonal changes in wind direction are accompanied by dramatic shifts in precipitation regime between very dry and very rainy. Nowhere is this phenomenon more dramatically displayed than in the Asian monsoon.

During summer the Tibetan plateau is heated by insolation, and much of this energy is transferred to the atmosphere, which warms significantly, leading to a reduction in surface pressure. The low surface pressure encourages a low-level flow of warm, moist air from the ocean to the land (Fig. 6.20), which supports intense precipitation over India and the slopes of the Himalayas during summer, particularly where the summer monsoon winds intersect with the mountains of western India and the Himalayas (Fig. 6.21). A similar encroachment of summertime precipitation occurs over eastern Asia. The heating by insolation and latent heat release drives upward motion in the atmosphere, which is necessary to balance the convergence of air at low levels. The seasonal movement of the main precipitation regions can be seen clearly in the OLR (Fig. 2.11). During winter the situation is reversed. The Himalayas cool dramatically, air flows toward the Indian Ocean from the land at low levels, and India and surrounding lands experience a wintertime drought (Fig. 6.21). The wind shift is particularly strong in the western Indian Ocean, and this causes a strong response in the ocean and the sea surface temperature (Fig. 7.9).

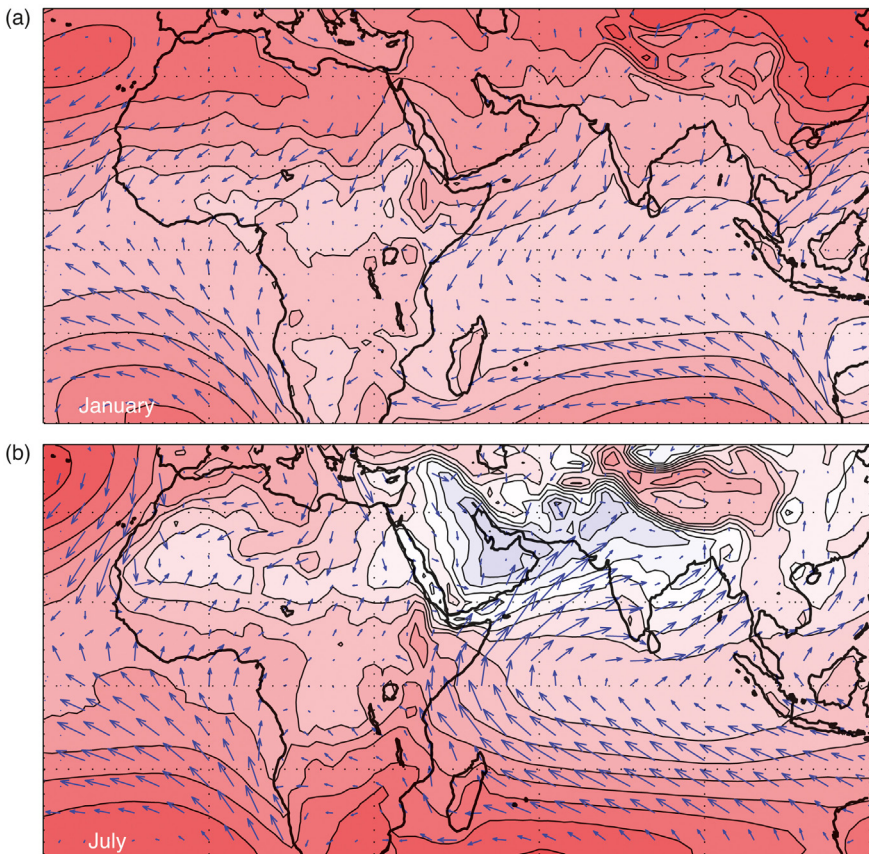


**FIGURE 6.20** Same as Fig. 6.19 except for the Afro-Asian monsoon region from 30°S to 40°N and 30°W to 120°E in mercator projection.

The switch from dry to moist conditions occurs abruptly at the time of summer monsoon onset, typically around the middle of June. The date of monsoon onset and the duration and intensity of rainfall during the rainy season vary from year to year. These fluctuations in summer precipitation can produce either flood or drought, and are of great importance for the populace in the regions affected.

### 6.5.2 Desert Climates

Desert climates occur in land areas where the precipitation is significantly less than the potential evapotranspiration, so that the surface becomes dry. Precipitation will generally occur where humid air is uplifted. Aridity can be caused by a variety of mechanisms, which are all associated

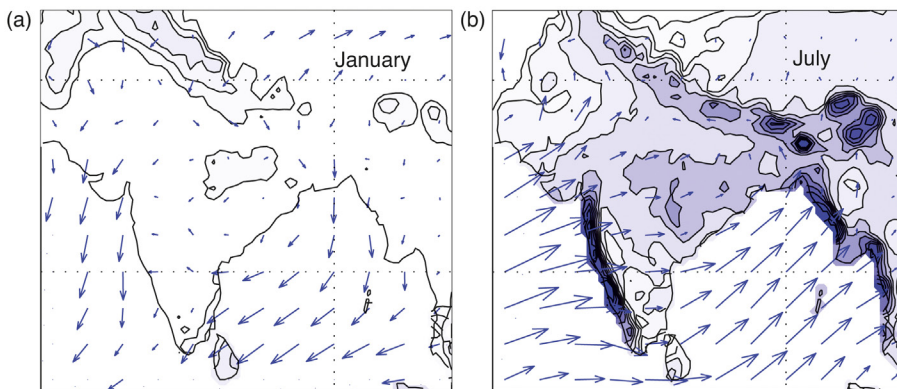


**FIGURE 6.21** Precipitation contours and 1000 hPa wind vectors over Southern Asia during (a) January and (b) July. Contours of precipitation are 20, 40, 80, 160, 320, 480... mm month<sup>-1</sup>. Data from GPCP v6 and ERA Interim.

with the circulation of the atmosphere. Rainfall can be suppressed by widespread, persistent subsidence associated with the general circulation of the atmosphere. As we have seen, the Hadley circulation implies downward air motions along much of the belt from about 10° to 40° latitude in both hemispheres, where many of the world's great deserts are found (Fig. 6.22). Regions of localized subsidence associated with mountain ranges can also lead to deserts. Persistent subsidence generally occurs on the downwind side of mountain ranges that stand athwart the prevailing wind direction. Examples are the North American Desert, which is downwind of the Cascade, Sierra, or Rocky Mountains, and the Monte and

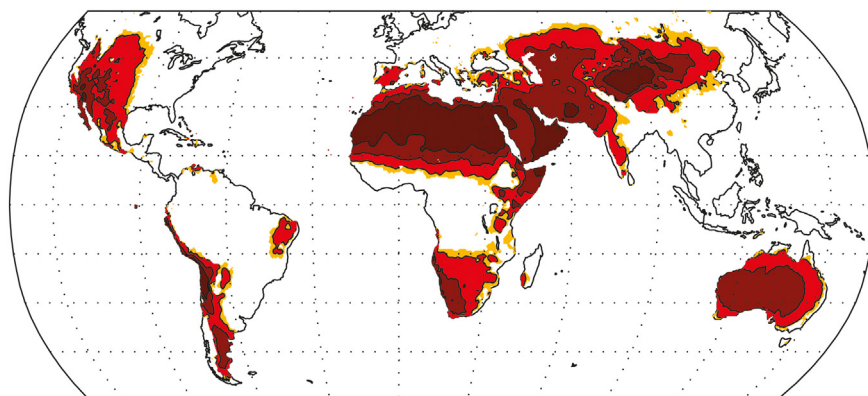


**FIGURE 6.22** Global distribution of dry lands defined as the ratio of precipitation to potential evapotranspiration (P/PET). Darkest red indicates most extreme aridity. Data from Feng and Fu (2013).

Patagonian deserts, which are to the east of the Andes Mountains in South America. The coastal deserts of Peru and Chile result from three causes: the large-scale subtropical subsidence, the localized subsidence associated with easterly flow over the Andes, and the cold sea surface temperatures adjacent to the deserts. When warm air flows over cold ocean surfaces, the air near the surface is cooled by sensible heat exchange and the atmosphere becomes stable to moist convection, because cold, dense air near the surface cannot easily rise through the warmer air above.

Deserts may also be formed in regions that are blocked from a supply of humid air. If air is forced to cross a mountain range, its humidity is greatly reduced as the air stream is uplifted on the windward side. As the air rises, it cools, and the water vapor condenses to form heavy precipitation. On the leeward side, the air sinks and warms, giving the air an extremely low relative humidity. The deserts of central Asia, such as the Gobi, occur in regions that are either very distant from the ocean or separated from the ocean by a major mountain range. The Sahara and Arabian (Rub'al Khali) deserts constitute one of the largest and most arid regions on Earth. This results from their large land mass and their position in the subtropics where mean air motions are downward and insolation is large. Because of their high surface temperature and high albedo, these deserts are regions of net radiation loss in the annual average (Fig. 2.12). The atmospheric circulation provides energy to these regions by import of high-energy air at high levels of the atmosphere. The air then subsides over the deserts as it radiatively cools. The outflow of this air at low levels exports moisture and helps to sustain the great dryness of these regions.

All deserts share a very dry surface and precipitation much lower than the potential evaporation, but can vary greatly in their mean temperatures. For example, Ouallen, Algeria, a town in the Sahara at 22.8°N, 5.53°E, has a maximum monthly mean temperature of 38°C in July, a minimum of 16°C in January, and an annual precipitation of about 22 mm. In contrast, Antofagasta, Chile in the coastal Atacama Desert at 23.5°S, 70.4°W, has an even lower annual precipitation of 2 mm, but has much colder temperatures. Antofagasta has a monthly mean maximum temperature of 20°C in January and a minimum of 13°C in July. The coastal Peruvian and Atacama deserts are remarkable because the low temperatures and frequent stratus cloud and fog associated with the cold temperatures of the adjacent ocean are juxtaposed with an extreme lack of precipitation.

Most deserts have a large diurnal variation in surface temperature, because the surface warms substantially during the day in response to insolation, and cools rapidly at night because longwave radiation emitted by the surface exceeds the downward longwave coming from the dry, cloudless atmosphere. Deserts at high altitude experience an even greater diurnal cycle, because the atmospheric greenhouse effect is weak. Seasonal variations of temperature can also be rather large in mid-latitude

arid lands, with freezing temperatures in winter and very hot daytime temperatures in summer.

### 6.5.3 Wet Climates

Wet climates occur where the precipitation is heavy and exceeds the evapotranspiration for much of the year. Tropical wet climates are supported by the natural tendency of the atmospheric circulation to bring warm moist air to the equator. Islands that fall under the ITCZ are favored by heavy rainfall, and all of the major tropical landmasses have a region with a wet climate near the equator. The major regions of convection and precipitation in the tropics can be seen in the seasonal means of OLR in Fig. 2.11. Along the equator, three minima in the OLR are associated with rainy regions over South America, Africa, and the Indonesian–western Pacific region. These zones of heavy precipitation move north and south with the seasons and tend to occur in the summer hemisphere. The regions of lowest seasonal mean OLR occur where the most extensive upper-level clouds exist (Fig. 3.20), and these clouds are in turn representative of intense convection and rainfall.

The combination of equatorial location, shallow seas, and relatively small landmasses in the region of Malaysia, Indonesia, and New Guinea gives rise to the biggest region of intense precipitation on Earth. Here high sea surface temperatures and strong solar forcing of diurnal land–sea breezes around the many islands foster frequent intense convection and precipitation. This large region of intense convection provides a strong thermal forcing for the large-scale circulation of the tropical atmosphere. The seasonal movement in the mass of convection centered over Indonesia has both north–south and east–west components. During Southern Hemisphere summer, the convection extends southeastward over the South Pacific Ocean and is identifiable as far away as 30°S, 140°W (Fig. 5.4). This feature is called the *South Pacific convergence zone* (SPCZ). During Northern Hemisphere summer, the SPCZ is retracted back across the dateline, and the Indonesian convection extends northwestward into the Bay of Bengal, where it becomes connected with the convection associated with the Asian summer monsoon.

The largest area of tropical rain forest exists in the Amazon Basin of South America. The Amazon Basin receives more than 2 m of precipitation per year. The heavy precipitation over the vast area of the Amazon Basin is favored by the basin’s equatorial location and its orientation in relation to the prevailing easterlies of the tropical atmosphere. Northeasterly winds carry large amounts of water vapor into the Amazon Basin from the Atlantic Ocean. The westward flow of moist air is unimpeded by the very gradual slope of the basin until the barrier formed by the Andes Mountains at the western extremity of the basin prevents the water vapor from simply flowing across South America without precipitation. Once convection is initiated over the Amazon Basin, the resulting latent heat release drives upward

motion in the atmosphere, rain that falls on the surface can be recycled as further rain and further inflow of humid air from the east can occur at low levels. A circulation of this nature is capable of delivering large amounts of precipitation to the surface of the basin and supports a huge volume of surface runoff to the Amazon River, which has the largest flow of any river in the world. Away from the Equator rainfall is seasonal, however, and is greatest in the summer hemisphere, so that the rainy seasons on opposite sides of the equator tend to occur 6 months apart (Fig. 6.23).

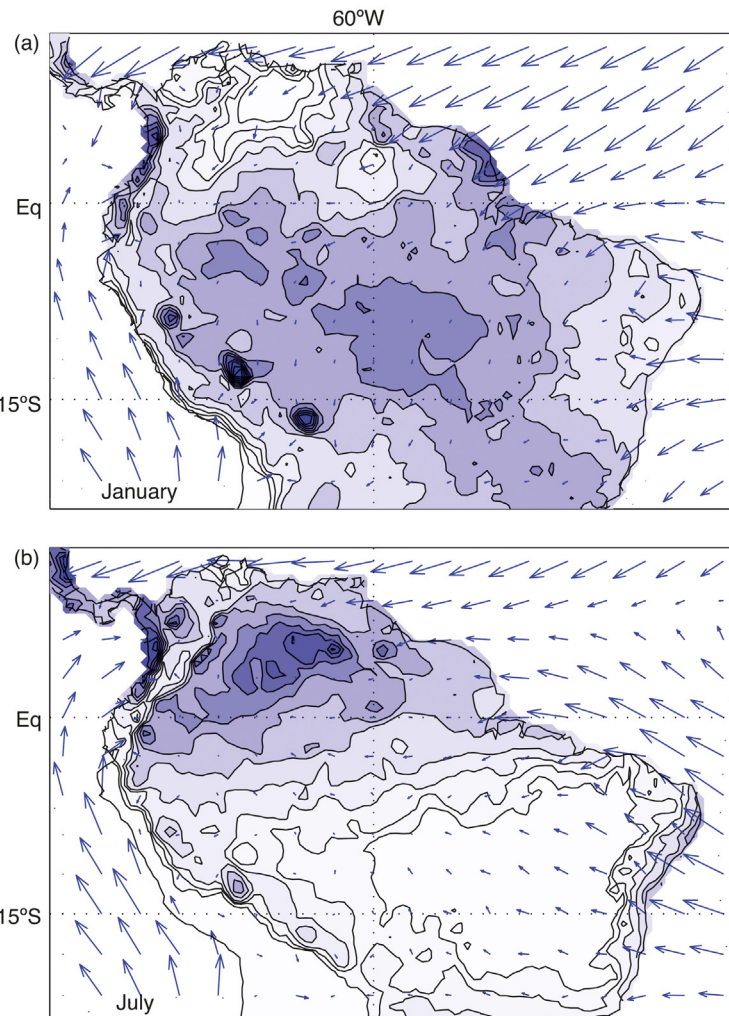


**FIGURE 6.23** Seasonality and annual mean of precipitation and 1000 hPa winds over tropical South America. Contours of precipitation are 10, 20, 40, 80, 160, 240... mm month<sup>-1</sup>. Data from GPCP v6 and ERA Interim.

### 6.5.4 Tropical Wet and Dry Climates

Many tropical regions have a wet season and a dry season of varying lengths. An interesting example that covers a very large area is the northern half of Africa, where the climate varies from wet near the equator to extremely arid at 25°N, with the southern boundary of the Sahara Desert roughly along 16°N. Between these two extremes the precipitation is seasonal, with a wet period and a dry period (Fig. 6.24). The precipitation and low-level convergence are tied together and follow the insolation into the summer hemisphere. Figure 6.20 shows that during July the pressure drops over the central Sahara and winds along 15°N come from the southwest, bringing moist air toward the Sahara, just the reverse of during January. During summer, strong solar heating of the surface results in a transfer of heat to the air, which can support mean upward motion. This upward

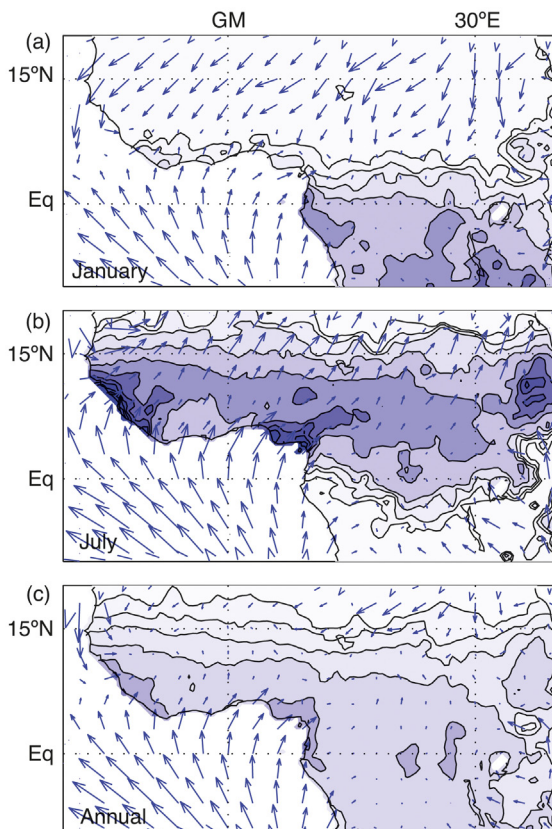


**FIGURE 6.24** Seasonality and annual mean of precipitation and 1000 hPa winds over tropical Africa. Contours of precipitation are 10, 20, 40, 80, 160, 240... mm month<sup>-1</sup>. Data from GPCP v6 and ERA Interim.

motion can draw moist, low-level air from the south that has its origin in the Gulf of Guinea or in the moist land areas of central Africa. As a result, precipitation in the semiarid lands at the southern margin of the Sahara Desert occurs only during the summer season, when solar heating of the surface is sufficient to drive upward motion and low-level convergence there. In the tropical Western Sahara during July, the minimum sea-level pressure and apparent low-level convergence occur near 22°N, 5°W (Fig. 6.20). However, the precipitation associated with this low-level convergence is quite small, because the air must follow a long trajectory over warm and dry land areas so that it is quite dry when it reaches the area where the low-level winds converge and support shallow rising motion. The low-level wind convergence during January occurs at about 7°N in western Africa, which is much closer to the moisture source in the Atlantic Ocean (Fig. 6.24), and which therefore produces very heavy precipitation. During July, the wind convergence in Western Africa extends to 10°N where the winds become weak in the region of heavy precipitation, but they then accelerate toward the low pressure center farther north. Along the southern coast of western Africa the precipitation peaks twice a year during early summer and late fall. This double maximum is associated with the Sun being exactly over the equator twice a year. Precipitation is stronger in all seasons in the highlands of Ethiopia at around 10°N and 40°E.

The wet season in Africa decreases in duration and reliability as one moves northward from the equator. Figure 6.25 shows the progression from desert, to savanna to tropical wet climate as one travels south from the Sahara toward the equator. As a general rule, the fractional variation of precipitation from year to year increases as the mean annual precipitation decreases, so lands that have low precipitation also have a high probability of unusually dry or wet years. At the southern margin of the Sahara Desert, in a region often called the Sahel, life is particularly sensitive to failures of the summer rainfall, especially when the rains fail for several years in succession as they did in 1910–1913, 1938–1942, and 1969–1973. Drought periods in the Sahel have been related to decadal changes in sea surface temperature, and may be made worse by the local environmental changes induced by humans and their domestic animals. Domestic animals such as goats and cattle need vegetation to eat, and humans need firewood for cooking. If the density of human and animal populations is such that the land is denuded of vegetation, then the desert may advance into regions that were previously semiarid.

Changes in surface environment of arid lands can be very long lasting. When the rains fail and the surface vegetation is removed, the dominant surface covering may become windblown sand, which has a higher albedo than a vegetated surface. Such a surface will reflect more of the insolation,



**FIGURE 6.25** Three photographs showing the variation of surface conditions from the subtropical Sahara Desert to the ITCZ. (a) The Saharan oasis of Ghardaia, Algeria at 32°N. The water table approaches the surface in this depression so that date palms can be grown by irrigation. The annual rainfall is about 75 mm and the surrounding land is barren of vegetation. (b) Sahel region grassland between Agadez and Tanout, Niger at 16°N. The annual rainfall is about 400 mm. (c) Equatorial rain forest on the rim of the Congo Basin near Bondo, Zaire at 4°N. Annual rainfall is about 1800 mm. *Photos courtesy of S. G. Warren.*

(c)



FIGURE 6.25 (Cont.)

so that the heating rate necessary to drive low-level convergence may not be attained, and the rains will be more likely to fail. The reverse feedback process is also possible. Random weather events or the remote influence of sea surface temperature changes can lead to a succession of wet years. A few years of enhanced rainfall can foster the development of surface vegetation that will hold down the sand and decrease the surface albedo, thereby increasing the probability of additional wet years. The desert margin is thus a sensitive region, and can be altered by modest forces driving it toward greater or lesser aridity. Paleoclimatic evidence presented in Chapter 8 shows that the Sahara was not always a desert, and that natural changes can transform its climate to a much wetter one.

---

## EXERCISES

1. Discuss why the net energy transport of the Hadley circulation is much less than the poleward transport of potential energy. In what ways are the Hadley circulation and its energy transports related to the climate of the tropics?
2. Draw Fig. 6.7 for the Southern Hemisphere using the same coordinate axes. Make sure that what you draw transports heat and momentum toward the South Pole.
3. Derive (6.19) from (6.15) and (6.13).

4. Calculate the zonal velocity of an air parcel at the equator, if it has conserved angular momentum while moving to the equator from 20°S, where it was initially at rest relative to the surface.
5. The tropical easterlies and mid-latitude westerlies occupy about the same surface area of Earth. Would you expect the surface westerly winds to be stronger, weaker, or about the same as the surface easterlies? Explain your answer with equations.
6. Estimate the rate at which air must subside over the Sahara to balance the heat loss by radiation shown in Fig. 2.11a. (*Hint:* Approximate the vertical gradient of moist static energy with that of potential energy and then use downward advection against this gradient to balance a radiative heat loss, for example,  $w \partial(gz) / \partial z = R_{\text{TOA}} \times (p_s / g)^{-1}$ .)
7. It has been speculated that you might be able to bring rainfall to the Sahara by decreasing the surface albedo. Estimate how much the albedo of the Sahara would need to decrease in order to convert its current net annual loss of radiation to a net annual gain of radiation of the same magnitude. This net radiative heating could support mean upward motion that would produce precipitation. How can you account for the likely surface temperature increases and associated longwave energy loss increases that will occur if you increase the solar absorption without providing moisture for evaporation?
8. Using the results of problems 6 and 7 and the tropical humidity distribution in Fig. 1.9, estimate how much albedo decrease you would need to generate net radiative heating to drive mean vertical motion sufficient to produce runoff from the Sahara equivalent to 1 m of precipitation per year. (*Hint:* Equate the vertical transport of water vapor at the top of the boundary layer with the precipitation rate  $P$ , for example,  $(w\rho_a q)_{1\text{ km}} = P\rho_w$ , where  $\rho_a$  and  $\rho_w$  are the density of air and liquid water, respectively, and  $q$  is the mass mixing ratio of water vapor. Compare your result with the net radiation over the Amazon Basin during the rainy season (Fig. 2.11)).